



Effect of cutout on stochastic natural frequency of composite curved panels



S. Dey ^a, T. Mukhopadhyay ^{b, *}, S.K. Sahu ^c, S. Adhikari ^b

^a Mechanical Engineering Department, National Institute of Technology Silchar, India

^b College of Engineering, Swansea University, Swansea, United Kingdom

^c Department of Civil Engineering, National Institute of Technology Rourkela, India

ARTICLE INFO

Article history:

Received 21 June 2016

Received in revised form

29 July 2016

Accepted 19 August 2016

Available online 31 August 2016

Keywords:

Cutout

Composite

Support vector regression

Random natural frequency

Uncertainty quantification

Noise

ABSTRACT

The present computational study investigates on stochastic natural frequency analyses of laminated composite curved panels with cutout based on support vector regression (SVR) model. The SVR based uncertainty quantification (UQ) algorithm in conjunction with Latin hypercube sampling is developed to achieve computational efficiency. The convergence of the present algorithm for laminated composite curved panels with cutout is validated with original finite element (FE) analysis along with traditional Monte Carlo simulation (MCS). The variations of input parameters (both individual and combined cases) are studied to portray their relative effect on the output quantity of interest. The performance of the SVR based uncertainty quantification is found to be satisfactory in the domain of input variables in dealing low and high dimensional spaces. The layer-wise variability of geometric and material properties are included considering the effect of twist angle, cutout sizes and geometries (such as cylindrical, spherical, hyperbolic paraboloid and plate). The sensitivities of input parameters in terms of coefficient of variation are enumerated to project the relative importance of different random inputs on natural frequencies. Subsequently, the noise induced effects on SVR based computational algorithm are presented to map the inevitable variability in practical field of applications.

© 2016 Elsevier Ltd. All rights reserved.

1. Introduction

Composite panels are employed in a plentitude of shallow weight-sensitive load bearing structural components for wide range of aerospace, automotive, nuclear, marine and civil engineering applications. The cutouts of composite panels are inevitable primarily for practical considerations. These are generally utilized not only to access ports for mechanical and electrical systems, but also to serve as doors and windows. Moreover, it is employed for inspection or maintenance purposes of the system. The dynamic behavior composite laminates may fluctuate significantly due to presence of cutout. In other words, the free vibration characteristics of composite curved panels are affected due to variability in shape, size and location of cut outs. Its effects are more difficult to quantify when such composite panels are subjected to random oscillations with uncertain geometric and material

properties. The combined effect of cutout along with different stochastic material and geometric parameters may cause wide range of uncertainty in vibration behavior of the structure which may lead to sudden failures due to resonance. It is essential to quantify the uncertain natural frequencies of such composite structural components accurately and thereby follow a design process accounting all the uncertainties appropriately. Composite structures have more uncertainties and variabilities in the structural properties than conventional structures because of large number of structural parameters (inter-dependent in nature) and complex manufacturing and fabrication processes leading to less overall design control. In order to have more exact and realistic analysis, they can be modelled as stochastic structures i.e., structures with uncertain system parameters (both in inputs and outputs). Beside these, the inherent errors involved in finite element modelling lead to inaccuracy in results. A brief review of the literature dealing with the effect of cutout in composite laminates and stochastic analysis of general composite structures is presented in the next paragraph.

A detail bibliography of previous investigations on dynamics of composite plates with cutouts is given in review papers [1–3]. The

* Corresponding author.

E-mail address: 800712@swansea.ac.uk (T. Mukhopadhyay).

URL: <http://www.tmukhopadhyay.com>

past investigations [4–9] incorporating cutouts are primarily confined to buckling and free vibration analysis of composite plates in a deterministic framework. Thornburgh and Hilburger [10] carried out both experimental as well as numerical studies of composite panels with cutouts subjected to compressive load while Dimopoulos and Gantes [11] employed the numerical methods to design the cylindrical steel shells with cutouts. The deterministic free vibration analyses of laminated composite shells with cutout are studied by many researchers [12–18]. The mode shapes and natural frequencies are investigated for cross-ply laminates with square cut-outs by Jenq et al. [19]. Eiblmeier and Loughlan [20] studied on buckling analysis of composite panels with circular shaped cut-outs. Sivakumar et al. [21] considered large amplitude oscillation on frequency analyses of composite plates with cutout. In past, multi-dimensional deterministic studies are carried out to conduct investigations on behavior of composite and sandwich plate or shells with cutouts such as Anuja and Katukam [22] presented parametric studies on the cutouts in heavily loaded aircraft beams, Mondal et al. [23] studied the dynamic performance of sandwich composite plates with circular hole. Recently Venkatachari et al. [24] investigated on influence of environment for free vibration of composite laminates with cutouts and Yu et al. [25] studied on buckling and free vibration analyses of laminated composites plates with complicated cutouts employing first order shear deformation theory and level set method. Plenty amount of research is carried out on free vibration analysis of composite plates, shells and sandwich structures [26–40]. A concise review of literature on application of efficient reduced order models in the field of structural analysis and design is presented next. Ample research is conducted on response surface methodologies in conjunction to composite materials in past, such as, Park et al. [41/29] conducted a numerical investigation on composite shells employing stochastic finite element method (SFEM) while Zhao et al. [42] investigated on material behavior modelling with multi-output support vector regression. Recently, Zhigang et al. [43] incorporated a response surface method (RSM) to analyze the reliability of turbine blades made of composites. Nik et al. [44] conducted an illustrative study of metamodelling methods in conjunction to design optimization of composites subjected to variable stiffness, while Steuben et al. [45] carried out the inverse characterization of composite materials by surrogate modelling. Some researcher employed the perturbation-based stochastic multi-scale analyses of composite materials [46,47]. Considering stochastic nonlinear systems, Gao and Tong [48] employed fuzzy to design composites while Kepple et al. [49] incorporated an improved stochastic method for buckling of composite cylindrical shells dealing with modelling errors.

Despite the engineering importance of cutouts involved in composites as pointed out in the preceding paragraphs, the number of research articles and reports in conjunction to the subject topic are found to be limited to deterministic results, possibly due to the computational complexity involved in it. The present study is focused to quantify the uncertain natural frequencies for composite panels with cutouts following an efficient support vector regression based algorithm in conjunction with finite element analysis. In general, the deterministic approach of finite element analysis becomes computationally inefficient and costly when the input parameters considered at each nodal points of each discretized element becomes random with respect to its meshing pattern and boundary condition. The number of elements depends not only on cutout-size but also on its shape and location. Moreover, due to random variability of each input parameters at element level throughout the structure, the application of identical isotropic plate elements for computing the element mass and stiffness matrices will never match with reality. Thus

uncertainty quantification for such structures following traditional Monte Carlo simulation based approaches is prohibitively expensive because of the fact that the exorbitant numbers of finite element iterations are required for separate random input parameter sets. This complex problem of composites can be effectively handled by using Support Vector Regression (SVR) which is employed as an efficient surrogate of the expensive finite element model allowing rigorous occurrence of virtual iterations to be exercised with cost-effectiveness. In stochastic structural problems, it can be restricted to consideration of the two-class problems, namely, with linear and non-linear classifier, without loss of generality. In such problems, the aim is to segregate the two classes by means of a function which is induced from known random dataset. In other words, the prime objective is to produce a classifier that will work well on unpredictable random data, i.e. it generalizes well. The conformity of such phenomenon can be efficiently dealt by SVR model. Due to inherent complexity, composite structures have intrusive variability of geometric and material properties in both linear and nonlinear domain while analyzing the structural reliability. Moreover the risk involved in ensuring the reliability of such system can be projected as the accidental loss plus uncertain measure of such loss. In compliance of the same, the present study aimed to predict those uncertain natural frequencies by employing support vector regression model. No literature is found which dealt with uncertainty quantification of natural frequencies in laminated composite panels with cutout using the support vector regression model. The random variation of individual parameters and combined parameters are considered in the present investigation. This article is organized hereafter as, section 2: stochastic finite element formulation for composite curved panels with cutout, section 3: brief description of support vector regression, section 4: support vector regression based uncertainty quantification algorithm for composite laminates with cutout including the effect of noise, section 5: results and discussion, section 6: conclusion.

2. Governing equations

In the present study, the composite panels with central cutout (as shown in Fig. 1) are considered. The stress resultants can be expressed in terms of the mid-plane strains and curvatures as

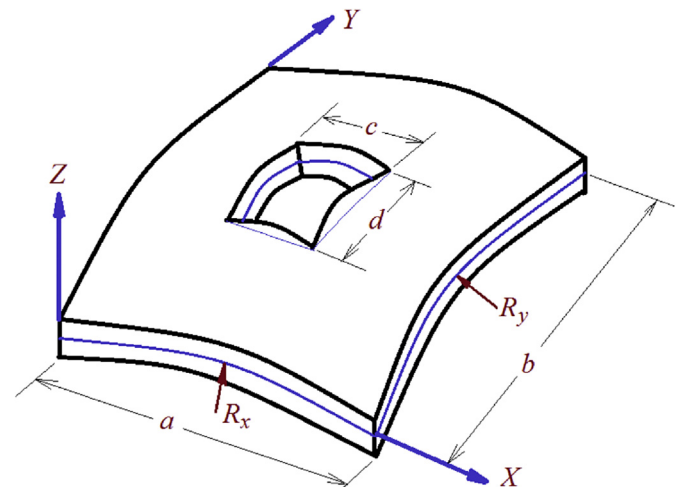


Fig. 1. Laminated composite curved panel with cutout.

$$\begin{Bmatrix} N_i(\bar{\omega}) \\ M_i(\bar{\omega}) \\ Q_i(\bar{\omega}) \end{Bmatrix} = \begin{bmatrix} A_{ij}(\bar{\omega}) & B_{ij}(\bar{\omega}) & 0 \\ B_{ij}(\bar{\omega}) & D_{ij}(\bar{\omega}) & 0 \\ 0 & 0 & S_{ij}(\bar{\omega}) \end{bmatrix} \begin{Bmatrix} \epsilon_j \\ \kappa_j \\ \gamma_j \end{Bmatrix} \quad (1)$$

The constitutive equation [50] is given by

$$\{F\} = [D(\bar{\omega})] \{\epsilon\} \quad (2)$$

Subsequently, extension, bending-stretching coupling and bending terms can be expressed as

$$\begin{aligned} [A_{ij}(\bar{\omega}), B_{ij}(\bar{\omega}), D_{ij}(\bar{\omega})] &= \sum_{k=1}^n \int_{z_{k-1}}^{z_k} [\{\bar{Q}_{ij}(\bar{\omega})\}_{on}]_k [1, z, z^2] dz \quad i, j \\ &= 1, 2, 6 \end{aligned} \quad (3)$$

The transverse shear term can be derived from

$$[S_{ij}(\bar{\omega})] = \sum_{k=1}^n \int_{z_{k-1}}^{z_k} \alpha_s [\bar{Q}_{ij}(\bar{\omega})]_k dz \quad i, j = 4, 5 \quad (4)$$

where $\bar{\omega}$ indicates the representation of randomness while α_s denotes the shear correction factor ($\alpha_s = 5/6$) and $[\bar{Q}_{ij}]$ are the off-axis elastic constant matrix for elements which can be expressed as

$$\begin{aligned} \bar{Q}_{11}(\bar{\omega}) &= Q_{11}(\bar{\omega})m^4 + 2[Q_{12}(\bar{\omega}) + 2Q_{66}(\bar{\omega})]m^2n^2 + Q_{22}(\bar{\omega})n^4 \\ \bar{Q}_{12}(\bar{\omega}) &= [Q_{11}(\bar{\omega}) + Q_{22}(\bar{\omega}) - 4Q_{66}(\bar{\omega})]m^2n^2 + Q_{12}(\bar{\omega})(m^4 + n^4) \\ \bar{Q}_{22}(\bar{\omega}) &= Q_{11}(\bar{\omega})n^4 + 2[Q_{12}(\bar{\omega}) + 2Q_{66}(\bar{\omega})]m^2n^2 + Q_{22}(\bar{\omega})m^4 \\ \bar{Q}_{16}(\bar{\omega}) &= [Q_{11}(\bar{\omega}) - Q_{12}(\bar{\omega}) - 2Q_{66}(\bar{\omega})]nm^3 + [Q_{12}(\bar{\omega}) - Q_{22}(\bar{\omega}) + 2Q_{66}(\bar{\omega})]mn^3 \\ \bar{Q}_{26}(\bar{\omega}) &= [Q_{11}(\bar{\omega}) - Q_{12}(\bar{\omega}) - 2Q_{66}(\bar{\omega})]mn^3 + [Q_{12}(\bar{\omega}) - Q_{22}(\bar{\omega}) + 2Q_{66}(\bar{\omega})]nm^3 \\ \bar{Q}_{66}(\bar{\omega}) &= [Q_{11}(\bar{\omega}) + Q_{22}(\bar{\omega}) - 2Q_{12}(\bar{\omega}) - 2Q_{66}(\bar{\omega})]m^2n^2 + Q_{66}(\bar{\omega})(m^4 + n^4) \end{aligned} \quad (5)$$

The off-axis elastic constant matrix linked with transverse shear deformation can be expressed as

$$\begin{aligned} \bar{Q}_{44}(\bar{\omega}) &= G_{13}(\bar{\omega})m^2 + G_{23}(\bar{\omega})n^2 \\ \bar{Q}_{45}(\bar{\omega}) &= [G_{13}(\bar{\omega}) - G_{23}(\bar{\omega})]mn \\ \bar{Q}_{55}(\bar{\omega}) &= G_{13}(\bar{\omega})n^2 + G_{23}(\bar{\omega})m^2 \end{aligned} \quad (6)$$

where $m = \sin \theta(\bar{\omega})$ and $n = \cos \theta(\bar{\omega})$, wherein $\theta(\bar{\omega})$ is random ply orientation angle. The on-axis terms can be represented as

$$\begin{aligned} [Q_{ij}(\bar{\omega})]_{on} &= \begin{bmatrix} Q_{11}(\bar{\omega}) & Q_{12}(\bar{\omega}) & 0 \\ Q_{12}(\bar{\omega}) & Q_{22}(\bar{\omega}) & 0 \\ 0 & 0 & Q_{66}(\bar{\omega}) \end{bmatrix} \quad \text{for } i, j = 1, 2, 6 \\ [\bar{Q}_{ij}(\bar{\omega})]_{on} &= \begin{bmatrix} Q_{44}(\bar{\omega}) & Q_{45}(\bar{\omega}) \\ Q_{45}(\bar{\omega}) & Q_{55}(\bar{\omega}) \end{bmatrix} \quad \text{for } i, j = 4, 5 \end{aligned} \quad (7)$$

Where

$$\begin{aligned} Q_{11} &= \frac{E_1(\bar{\omega})}{1 - \nu_{12}(\bar{\omega})\nu_{21}(\bar{\omega})} & Q_{22} &= \frac{E_2(\bar{\omega})}{1 - \nu_{12}(\bar{\omega})\nu_{21}(\bar{\omega})} & Q_{12} \\ &= \frac{\nu_{12}(\bar{\omega})E_2(\bar{\omega})}{1 - \nu_{12}(\bar{\omega})\nu_{21}(\bar{\omega})} \end{aligned}$$

$$Q_{66} = G_{12}(\bar{\omega}) \quad Q_{44} = G_{23}(\bar{\omega}) \quad Q_{55} = G_{13}(\bar{\omega})$$

In present study, the uniaxial in-plane periodic loads are considered for composite panel with cutout. The differential equations of equilibrium can be expressed as [51].

$$\begin{aligned} \frac{\partial N_x(\bar{\omega})}{\partial x} + \frac{\partial N_{xy}(\bar{\omega})}{\partial y} - \frac{1}{2}C_2 \left(\frac{1}{R_y(\bar{\omega})} - \frac{1}{R_x(\bar{\omega})} \right) \frac{\partial M_{xy}(\bar{\omega})}{\partial y} \\ + C_1 \left(\frac{Q_x(\bar{\omega})}{R_x(\bar{\omega})} + \frac{Q_y(\bar{\omega})}{R_{xy}(\bar{\omega})} \right) = P_1(\bar{\omega}) \frac{\partial^2 u(\bar{\omega})}{\partial t^2} + P_2(\bar{\omega}) \frac{\partial^2 \theta_x(\bar{\omega})}{\partial t^2} \end{aligned} \quad (8)$$

$$\begin{aligned} \frac{\partial N_{xy}(\bar{\omega})}{\partial x} + \frac{\partial N_y(\bar{\omega})}{\partial y} + \frac{1}{2}C_2 \left(\frac{1}{R_y(\bar{\omega})} - \frac{1}{R_x(\bar{\omega})} \right) \frac{\partial M_{xy}(\bar{\omega})}{\partial x} \\ + C_1 \left(\frac{Q_y(\bar{\omega})}{R_y(\bar{\omega})} + \frac{Q_x(\bar{\omega})}{R_{xy}(\bar{\omega})} \right) = P_1(\bar{\omega}) \frac{\partial^2 v(\bar{\omega})}{\partial t^2} + P_2(\bar{\omega}) \frac{\partial^2 \theta_y(\bar{\omega})}{\partial t^2} \end{aligned} \quad (9)$$

$$\begin{aligned} \frac{\partial Q_x(\bar{\omega})}{\partial x} + \frac{\partial Q_y(\bar{\omega})}{\partial y} - \frac{N_x(\bar{\omega})}{R_x(\bar{\omega})} - \frac{N_y(\bar{\omega})}{R_y(\bar{\omega})} - 2 \frac{N_{xy}(\bar{\omega})}{R_{xy}(\bar{\omega})} + N_x^0(\bar{\omega}) \frac{\partial^2 w(\bar{\omega})}{\partial x^2} \\ + N_y^0(\bar{\omega}) \frac{\partial^2 w(\bar{\omega})}{\partial y^2} = P_1(\bar{\omega}) \frac{\partial^2 w(\bar{\omega})}{\partial t^2} \end{aligned} \quad (10)$$

$$\frac{\partial M_x(\bar{\omega})}{\partial x} + \frac{\partial M_{xy}(\bar{\omega})}{\partial y} - Q_x(\bar{\omega}) = P_3(\bar{\omega}) \frac{\partial^2 \theta_x(\bar{\omega})}{\partial t^2} + P_2(\bar{\omega}) \frac{\partial^2 u(\bar{\omega})}{\partial t^2} \quad (11)$$

$$\frac{\partial M_{xy}(\bar{\omega})}{\partial x} + \frac{\partial M_y(\bar{\omega})}{\partial y} - Q_y(\bar{\omega}) = P_3(\bar{\omega}) \frac{\partial^2 \theta_y(\bar{\omega})}{\partial t^2} + P_2(\bar{\omega}) \frac{\partial^2 u(\bar{\omega})}{\partial t^2} \quad (12)$$

wherein C_1 and C_2 are represented as tracers of shear deformable version of the theories of Sanders ($C_1 = C_2 = 1$), Love ($C_1 = 1$ and $C_2 = 0$), and Donnell's ($C_1 = C_2 = 0$). $N_x(\bar{\omega})$, $N_y(\bar{\omega})$ and $N_{xy}(\bar{\omega})$ denote the stochastic in-plane stress resultants, $M_x(\bar{\omega})$, $M_y(\bar{\omega})$ and $M_{xy}(\bar{\omega})$ represents the stochastic moment resultants while $Q_x(\bar{\omega})$ and $Q_y(\bar{\omega})$ depict as the stochastic transverse shear stress resultants. $R_x(\bar{\omega})$, $R_y(\bar{\omega})$ and $R_{xy}(\bar{\omega})$ denote the stochastic radii of curvature along the x and y directions and the radius of twist, respectively.

$$(P_1, P_2, P_3)(\bar{\omega}) = \sum_{i=1}^n \int_{z_{k-1}}^{z_k} \rho_k(\bar{\omega}) [1, z, z^2] dz \quad (13)$$

where n is the layer number of laminate and $\rho_k(\bar{\omega})$ is the random

mass density of k -th layer; and z_k represents the k -th layer's distance from the midplane.

The present study considers eight nodes in isoparametric quadratic element wherein five degrees of freedom (three translations and two rotations) is assumed at each nodal point. Considering Hamilton's principle [52] in conjunction to Lagrange's equation, the dynamic equilibrium equation of motion for free vibration can be expressed as

$$[M(\bar{\omega})] \left[\ddot{\delta} \right] + [K(\bar{\omega})] \{ \delta \} = 0 \tag{14}$$

where $M(\bar{\omega})$, $[K(\bar{\omega})]$, $\{ \delta \}$ are represented as mass matrix, elastic stiffness matrix and vector of generalized coordinates. The random natural frequencies $[\omega_m(\bar{\omega})]$ are derived from the standard eigenvalue problem [53] using QR algorithm and are obtained as

$$\omega_m^2(\bar{\omega}) = \frac{1}{\lambda_m(\bar{\omega})} \quad \text{where } m = 1, 2, 3, \dots, n_m \tag{15}$$

where n_m denotes the mode number and $\lambda_m(\bar{\omega})$ indicates the m -th eigenvalue of matrix $A = K^{-1}(\bar{\omega})M(\bar{\omega})$.

3. Support vector regression

Support vector regression (SVR) model is derived from Support Vector Machine (SVM) pertaining to regression analysis. Suppose the training data is given as $\{(x_1, y_1), (x_2, y_2), \dots, (x_l, y_l)\} \subset \chi \times \Re$ where χ and \Re denote the space of the input patterns and Euclidean space vector. In support vector regression, the primary objective is to find a function $\hat{f}(x)$ that has at most ϵ deviation from the actually obtained targets y_i for all these training data and at the same time, is as flat as possible. The formulation In Fig. 2, only the points distributed outside the shaded zone are contributed to the cost linked with insensitive loss function (ζ) at points (m and n) wherein the deviations are penalized in a linear fashion. Thus the optimization problem is solved more easily in its dual formulation. Moreover, the dual formulation provides the key for extending SV machine to nonlinear functions. Hence it can be used as a standard dualization method utilizing Lagrange multipliers [54]. The errors are neglected as long as they are less than the region of tolerance (say $\pm\epsilon$) (refer to Fig. 2), but it will not accept any deviation larger than this limiting value. The SVR model is constructed by employing the subset sample data and support vectors wherein maximum deviation of ϵ from the function value of each training data exist. For a linear case, SVR model can be expressed as [55].

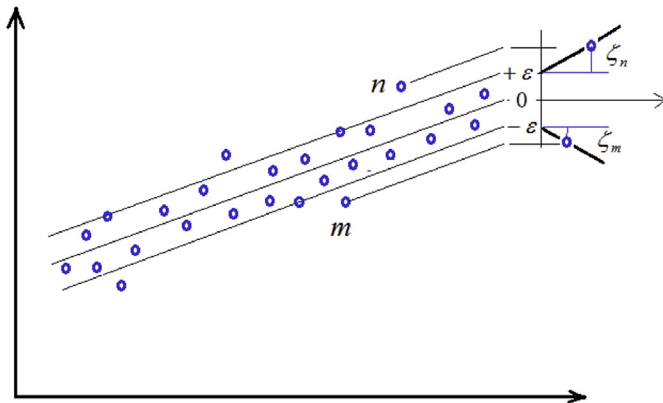


Fig. 2. Soft margin loss setting corresponding to a linear Support Vector machine [54].

$$\hat{f}(x) = \hat{Y}(x) = \langle W \cdot x \rangle + b \tag{16}$$

where $\hat{Y}(x)$, W and b indicate the predicted value of objective function, weight-vectors and bias, respectively while $\langle \cdot \rangle$ denotes the inner product. The sample data points within the $\pm\epsilon$ band (known as the ϵ -tube) are neglected, while the predictors are considered wherein the data points are found on or outside this region. The SVR prediction can be expressed as,

$$\hat{f}(x) = b + \sum_{i=1}^k W^{(i)} \psi(x, x^{(i)}) \tag{17}$$

where $\psi^{(i)}$ and $W^{(i)}$ are the basis function and weights, respectively. For generalized prediction, it is therefore needed to develop the function with ϵ deviations from y as well as least complex. Despite reducing the risk of using training data for fitting, SVR reduces the upper bound on the calculated risk by employing ϵ -insensitive loss function, as constrained convex quadratic optimization problem proposed by Ref. [51].

$$G(x) = \begin{cases} 0 & |Y(x) - \hat{Y}(x)| \leq \epsilon \\ |Y(x) - \hat{Y}(x)| - \epsilon & \text{Otherwise} \end{cases} \tag{18}$$

where ϵ and G parameters are selected based on the recommendation proposed by Cherkassky and Ma [56]. SVR model performs both linear as well as non-linear regression in conjunction to ϵ -insensitive loss function, simultaneously. It attempts to decrease the complexity by reducing the weighting vector as the objective function,

$$\begin{aligned} &\text{Minimize } \frac{1}{2} |W|^2 \\ &\text{Subjected to } \begin{cases} Y_i - \langle W \cdot x^{(i)} \rangle - b \leq \epsilon \\ \langle W \cdot x^{(i)} \rangle + b - Y_i \leq \epsilon \end{cases} \end{aligned} \tag{19}$$

A non-linear regression can be formed by replacing the $\langle \cdot \rangle$ in Eq. (16) with a kernel function, K as [57].

$$\hat{f}(x) = \sum_{i=1}^k (\alpha_i - \alpha_i^*) K(x_i, x) + b \tag{20}$$

In the present study, Gaussian kernel function is used throughout the entire investigation.

4. Stochastic approach using SVR model

The dimension of cutout of laminated composite panel with respect to each layer can be defined as $C_o = c/a$ where c/a denotes the percentage of cutout with respect to overall panel-dimension. The effects of both single variable as well as multi-dimensional random variables are investigated in conjunction to different sizes of cutout in the present analysis as follows:

- (a) Variation of only ply – orientation angle : $\theta(\bar{\omega})$
 $= \{ \theta_1 \theta_2 \theta_3 \dots \theta_i \dots \theta_l \}$
- (b) Variation of only twist angle : $\psi(\bar{\omega})$
 $= \{ \psi_1 \psi_2 \psi_3 \dots \psi_i \dots \psi_l \}$

(c) Variation of only thickness : $t(\bar{\omega}) = \{t_1 t_2 t_3 \dots t_i \dots t_l\}$

(d) Variation of only material properties : $p_m(\bar{\omega}) = \{p_{m(1)} p_{m(2)} p_{m(3)} \dots p_{m(i)} \dots p_{m(l)}\}$

(e) Combined variation of ply orientation angle, twist angle, thickness and materials properties : $g(\bar{\omega}) = \{\Phi_1(\theta_1 \dots \theta_l), \Phi_2(\psi_1 \dots \psi_l), \Phi_3(t_1 \dots t_l), \Phi_4(p_{m(1)} \dots p_{m(l)})\}$

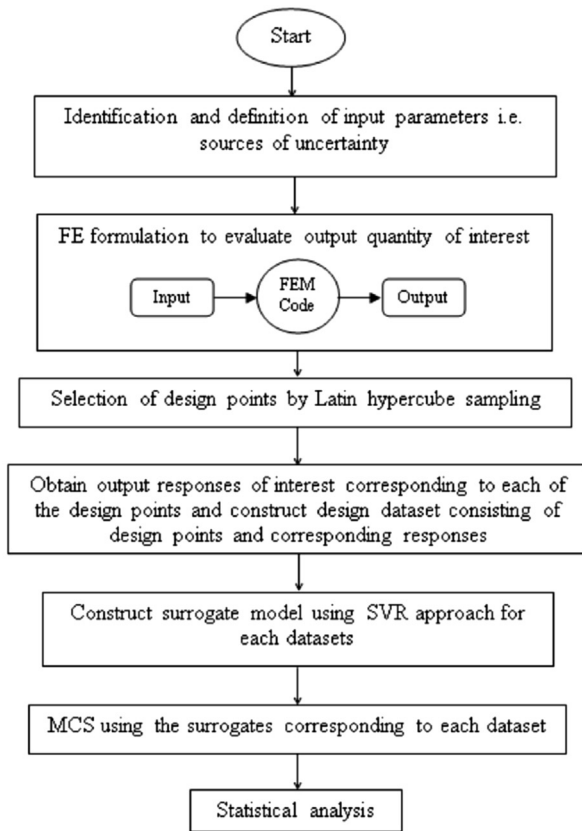
where for i th layer, $\theta_i, \psi_i, t_i, p_{m(i)}$ are the ply orientation angle, twist angle, thickness and material properties wherein material properties include $E_{1(i)}, E_{2(i)}, G_{12(i)}, G_{23(i)}, \mu_{12(i)}$ and ρ_i denoting the elastic modulus (longitudinal direction), elastic modulus (transverse direction), shear modulus (longitudinal direction), shear modulus (transverse direction), Poisson ratio and mass density, respectively (l is the total layer number, where $i = 1, 2, 3 \dots l$). In conformity of the same, $\pm 5^\circ$ variability is assumed for ply orientation and twist angle while $\pm 10\%$ variability from respective deterministic mean values of thickness and material properties are considered. The flowchart of uncertainty quantification algorithm based on SVR

with and without noise effect using SVR model is shown in Fig. 3. Latin hypercube sampling is used for forming the sample dataset of the input space.

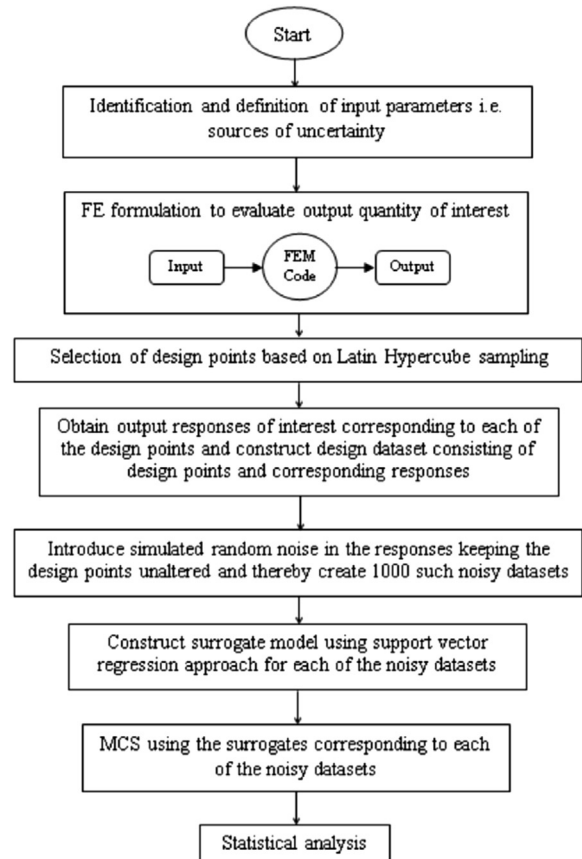
The pronounced noise-effect on the proposed SVR based UQ algorithm is also accounted by introducing different levels of noise as depicted in Fig. 3(b). In present investigation, Gaussian white noise is employed for SVR model formation

$$f_{ijN} = f_{ij} + p \times \xi_{ij} \tag{21}$$

where, p and f are the multiplication factor and natural frequency with the subscript i and j frequency number and sample number, respectively. A function generating random numbers (normal-distributed) with zero mean and unit standard deviation is represented as ξ_{ij} . Thus p (noise level) in the above expression basically represents the standard deviation of introduced noise level. Subscript N is used here to indicate the noisy frequency. Thus simulated noisy dataset (i.e. the sampling matrix for SVR model formation) is formed by introducing pseudo random noise in the



(a) SVR based uncertainty quantification algorithm without noise



(b) SVR based uncertainty quantification algorithm with noise

Fig. 3. Flowchart on uncertainty quantification algorithm based on SVR including the effect of noise.

Table 1

Convergence study for non-dimensional fundamental natural frequencies $[\omega = \omega_n L^2 \sqrt{(\rho/E_1 t^2)}]$ of three layered $(\theta^\circ/-\theta^\circ/\theta^\circ)$ graphite-epoxy untwisted composite plates ($a/b = 1$ and $b/t = 100$).

| θ | Present FEM | | | | | | | Ref. [64] |
|----------|-------------|---------|---------|-----------|-----------|-----------|-----------|-----------|
| | (4 × 4) | (6 × 6) | (8 × 8) | (10 × 10) | (12 × 12) | (16 × 16) | (20 × 20) | |
| 0° | 1.0112 | 1.0133 | 1.0107 | 1.0040 | 1.0031 | 1.0028 | 1.0022 | 1.0175 |
| 90° | 0.2553 | 0.2567 | 0.2547 | 0.2542 | 0.2540 | 0.2533 | 0.2530 | 0.2590 |

Table 2

Convergence of fundamental natural frequencies $(\lambda = \omega a^2 \sqrt{\rho h/D_{22}})$ of simply supported square plate with cutout size of $c/a = 0.5$, $a/b = 1$, $b/h = 100$.

| Shell type | Present FEM | | | | | Reddy [65] |
|-------------|-------------|---------|-----------|-----------|-----------|------------|
| | (4 × 4) | (8 × 8) | (12 × 12) | (16 × 16) | (20 × 20) | |
| Isotropic | 23.8432 | 23.570 | 23.4703 | 23.4364 | 23.4218 | 23.489 |
| Orthotropic | 51.8546 | 51.0597 | 50.7899 | 50.6944 | 50.6505 | 51.232 |
| Composite | 48.9546 | 48.2535 | 48.0650 | 48.0222 | 48.0064 | 48.414 |

responses, while the input design points are kept unaltered. Subsequently for each dataset, SVR based MCS is carried out to quantify uncertainty of composite laminates. The noise-effect is found to be investigated previously [58–62] for other problems and related to other surrogates. The assessment of SVR based uncertainty propagation with noise-effect is the first attempt of its kind to the best of authors' knowledge. The root-causes of such inevitable noise-effect can be attributed to the fact of other unknown sources of uncertainty such as measurement-errors, modelling-errors and computer simulation-errors and other system-specific epistemic

uncertainties. Thus the present investigation is portrayed with a comprehensive idea about the robustness of SVR based UQ algorithm including noise-effect.

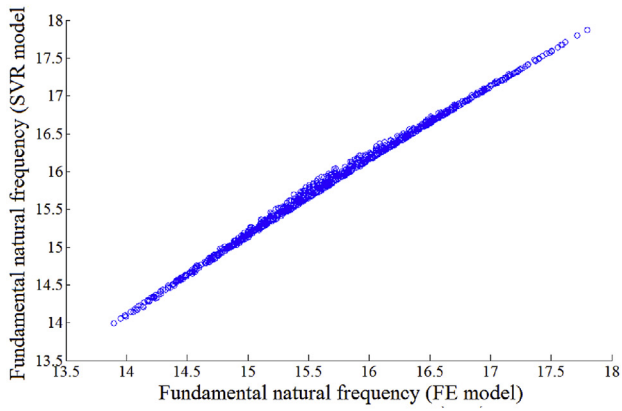
5. Results and discussion

The present study is dealt with three layered graphite-epoxy angle-ply composite cantilever spherical shallow panel with a central square shaped cutout. Four different types of panels are considered for detail analyses: plate ($R_x = R_y = \infty$), cylindrical ($a/$

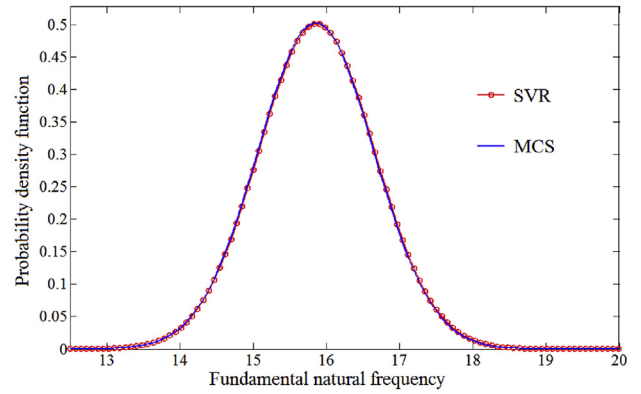
Table 3

Convergence study of natural frequencies corresponding to first three modes due to individual $[\theta (\bar{\omega})]$ and combined effect $[g(\bar{\omega})]$ of stochasticity for composite curved panels with cutout ($C_0 = 0.1$).

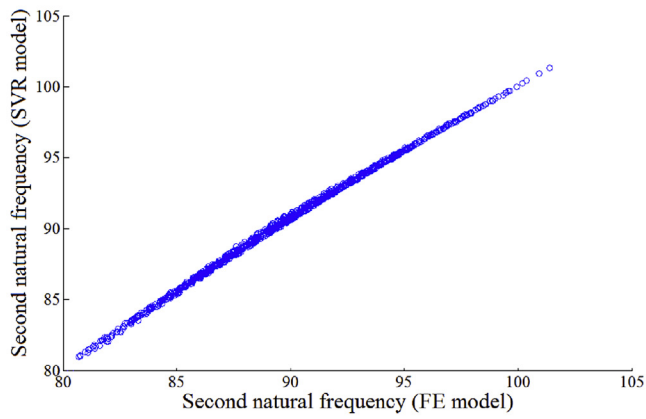
| Type | Mode | Method | Samples | Maximum | Minimum | Mean | SD |
|--|--------|----------------|---------|----------|----------|----------|---------|
| Individual variation (Only ply-orientation angle) | First | MCS | 10,000 | 17.8750 | 13.9750 | 15.8501 | 0.7935 |
| | | Present method | 64 | 17.8810 | 13.9782 | 15.8561 | 0.7948 |
| | | | 128 | 17.8604 | 13.9835 | 15.8464 | 0.7946 |
| | | | 256 | 17.8725 | 13.9905 | 15.8556 | 0.7929 |
| | | | 512 | 17.8770 | 13.9887 | 15.8570 | 0.7941 |
| | | | 1024 | 17.8758 | 13.9762 | 15.8512 | 0.7945 |
| | Second | MCS | 10,000 | 100.8807 | 79.8358 | 90.0001 | 4.2127 |
| | | Present method | 64 | 100.7124 | 80.99413 | 90.1040 | 4.1351 |
| | | | 128 | 100.6888 | 80.95801 | 89.9539 | 4.1981 |
| | | | 256 | 100.8305 | 80.01091 | 90.0567 | 4.2017 |
| | | | 512 | 100.8747 | 79.91743 | 90.0316 | 4.2215 |
| | | | 1024 | 100.8813 | 79.84141 | 90.0016 | 4.2301 |
| | Third | MCS | 10,000 | 136.1571 | 122.0387 | 128.9192 | 2.7264 |
| | | Present method | 64 | 136.1873 | 122.1453 | 129.9542 | 2.7171 |
| | | | 128 | 136.2222 | 121.9553 | 128.9793 | 2.7513 |
| | | | 256 | 136.1728 | 122.1545 | 129.9441 | 2.6950 |
| | | | 512 | 136.1651 | 122.0598 | 128.9398 | 2.7144 |
| | | | 1024 | 136.1578 | 122.0436 | 128.9291 | 2.7345 |
| Combined variation | First | MCS | 10,000 | 21.3550 | 13.1850 | 17.0607 | 1.3754 |
| | | Present method | 128 | 21.2290 | 13.2270 | 17.08304 | 1.3595 |
| | | | 256 | 21.4815 | 13.1062 | 17.07911 | 1.3963 |
| | | | 512 | 21.4277 | 13.1694 | 17.0867 | 1.3848 |
| | | | 1024 | 21.3673 | 13.1416 | 17.07897 | 1.3822 |
| | | | 2048 | 21.3778 | 13.1873 | 17.07107 | 1.3787 |
| | Second | MCS | 10,000 | 110.3002 | 73.0035 | 90.6014 | 6.4184 |
| | | Present method | 128 | 110.3709 | 72.9484 | 90.7125 | 6.3907 |
| | | | 256 | 110.9686 | 72.7500 | 90.6700 | 6.5456 |
| | | | 512 | 110.3437 | 73.1406 | 90.6806 | 6.4109 |
| | | | 1024 | 110.3767 | 73.0716 | 90.6662 | 6.4375 |
| | | | 2048 | 110.3034 | 73.0315 | 90.6418 | 6.4297 |
| | Third | MCS | 10,000 | 192.8565 | 123.9751 | 158.4033 | 14.0007 |
| | | Present method | 128 | 192.6459 | 124.6592 | 158.5274 | 13.9243 |
| | | | 256 | 193.2740 | 124.7608 | 158.6299 | 13.6715 |
| | | | 512 | 192.5198 | 124.5556 | 158.4206 | 13.8215 |
| | | | 1024 | 193.0577 | 124.1068 | 158.3772 | 13.9229 |
| | | | 2048 | 192.8565 | 123.9751 | 158.4033 | 14.0007 |



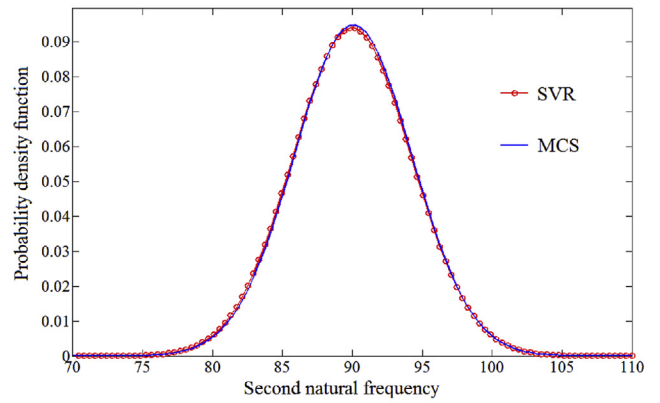
(a)



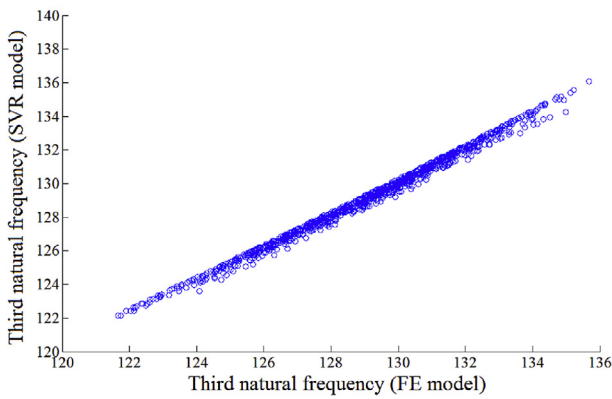
(b)



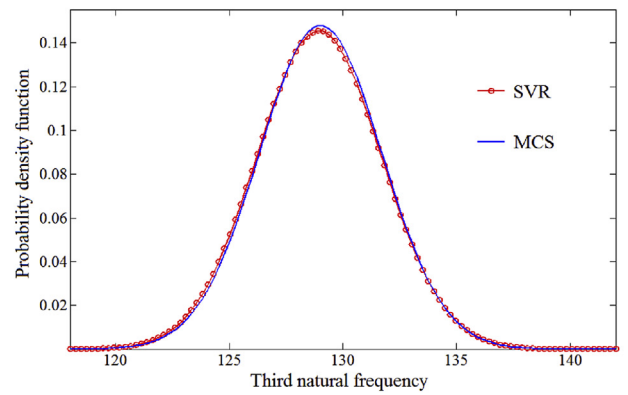
(c)



(d)

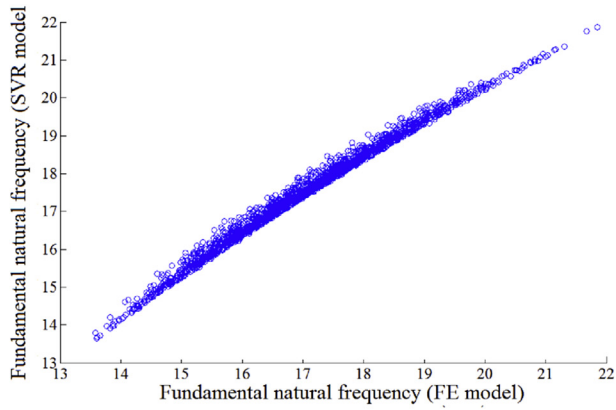


(e)

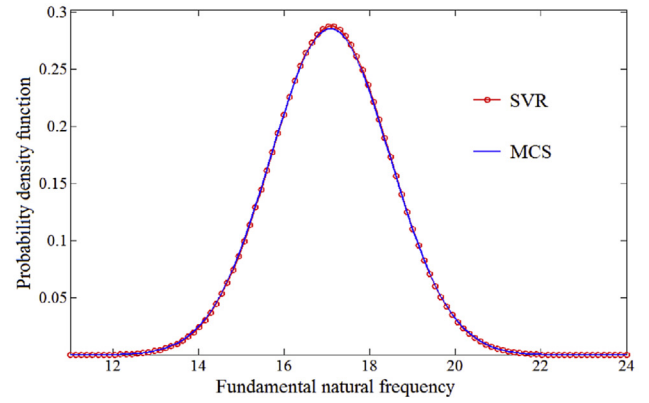


(f)

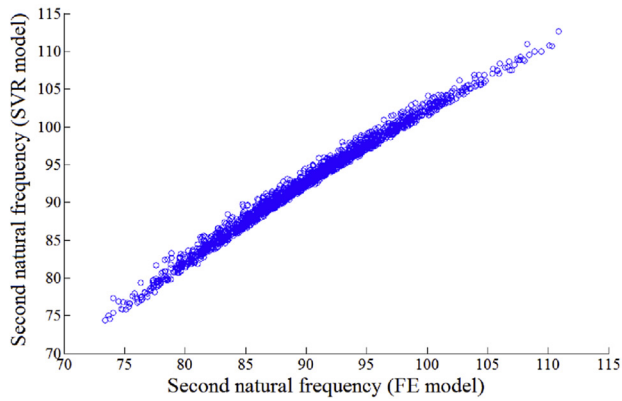
Fig. 4. (a, c, e) Scatter plot and (b, d, f) Probability density function plot for stochastic first three natural frequencies using SVR approach for individual variation of ply orientation angle $[\theta \ (\bar{\omega})]$ of angle-ply $(45^\circ/-45^\circ/45^\circ)$ composite curved panel with cutout ($C_0 = 0.1$).



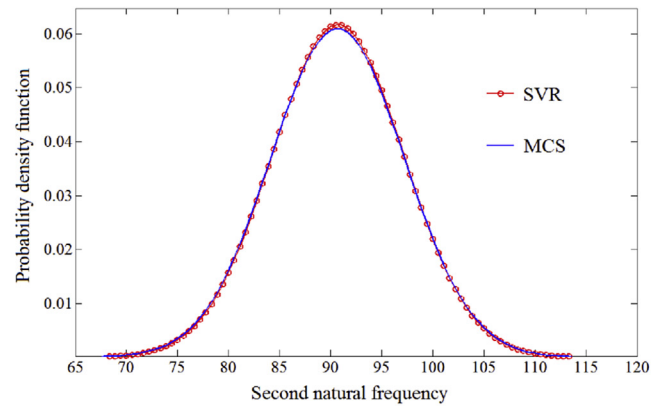
(a)



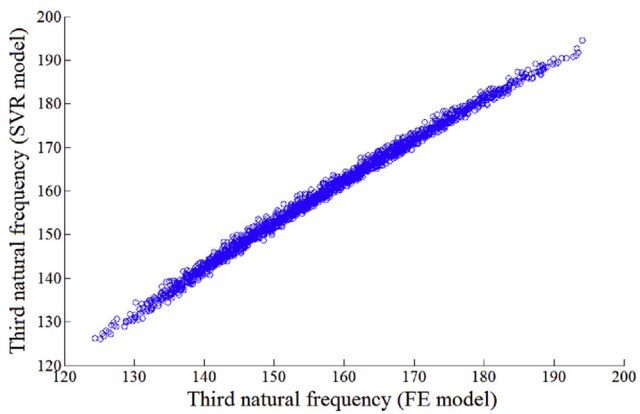
(b)



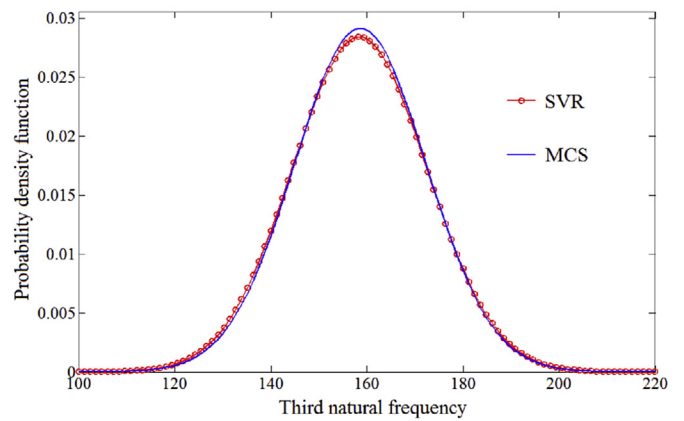
(c)



(d)



(e)



(f)

Fig. 5. (a, c, e) Scatter plot and (b, d, f) Probability density function plot for stochastic first three natural frequencies using SVR approach for combined variation of ply angle, elastic modulus, shear modulus, Poisson ratio and mass density $[g(\bar{\omega})]$ of angle-ply ($45^\circ/-45^\circ/45^\circ$) composite curved panel with cutout ($C_0 = 0.1$).

$R_x = \infty$, $b/R_y = 0.25$), spherical ($a/R_x = b/R_y = 0.25$) and hyperbolic paraboloid ($a/R_x = -0.25$, $b/R_y = 0.25$). The length, width and thickness of the composite laminate assumed in the present analyses are 1 m, 1 m and 5 mm, respectively and the dimension of the square shaped cutout size is considered as a percentage of its overall length and width [$C_l = c/a$ and $C_b = d/b$ wherein $c = d$ for square cutout] from 0.1 to 0.5 with a step of 0.1. Material properties of graphite–epoxy composite [63] are considered with deterministic mean values as $E_1 = 138.0$ GPa, $E_2 = 8.96$ GPa, $G_{12} = 7.1$ GPa, $G_{13} = 7.1$ GPa, $G_{23} = 2.84$ GPa, $\mu = 0.3$, $\rho = 1600$ kg/m³.

A convergence study is carried out to validate the present formulation and to ascertain the optimal finite element mesh size as shown in Tables 1 and 2. Table 1 presents the convergence study for non-dimensional fundamental natural frequencies of three layered graphite–epoxy untwisted angle-ply composite plates with finite element sizes (4 × 4), (6 × 6), (8 × 8) and (10 × 10), respectively in addition to comparison with the results obtained by Qatu and Leissa [64]. In contrast, Table 2 presents the convergence

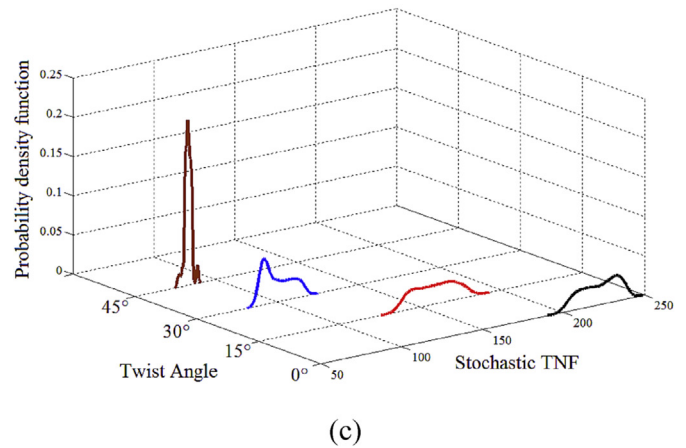
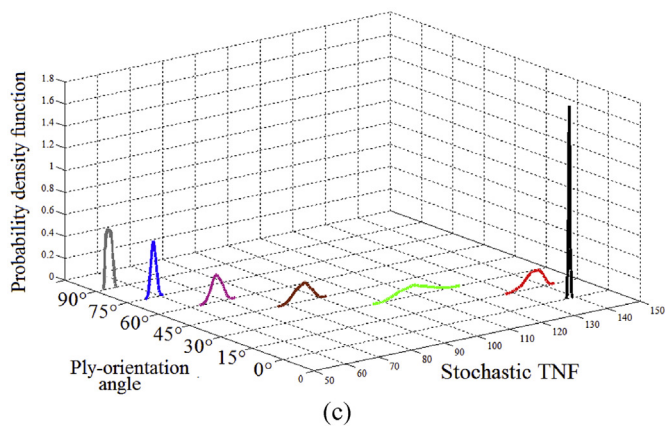
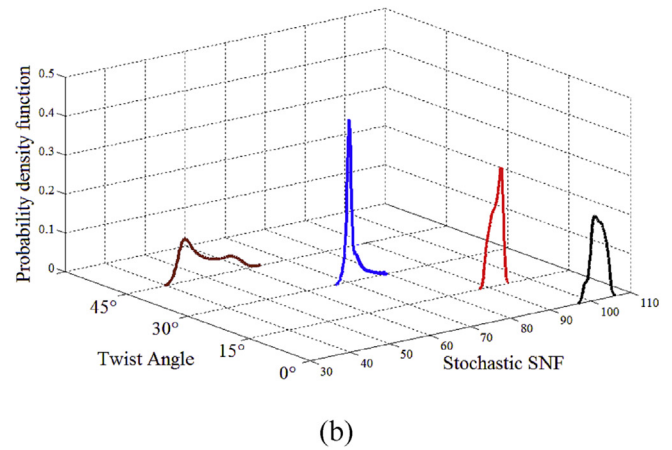
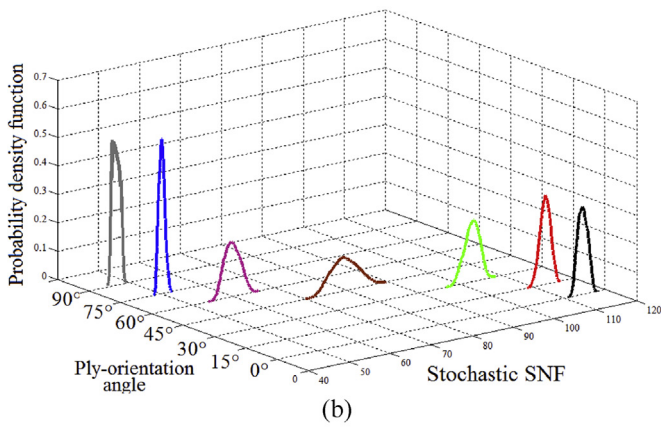
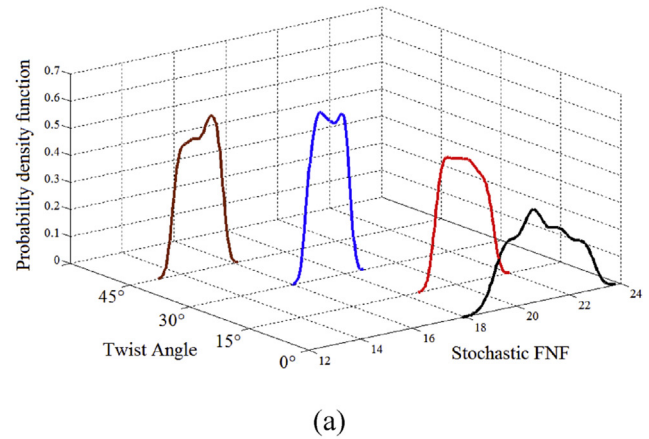
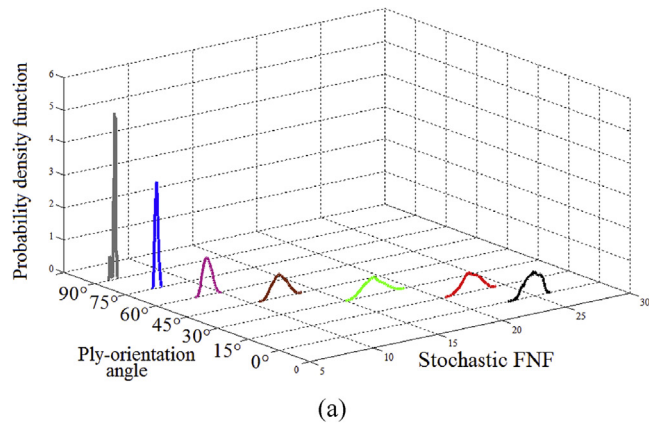


Fig. 6. Probability density function plot for first three stochastic natural frequencies using SVR approach for individual variation of ply orientation angle $[\theta (\bar{\omega})]$ of angle-ply ($\theta^\circ/-\theta^\circ/\theta^\circ$) composite curved panel with cutout.

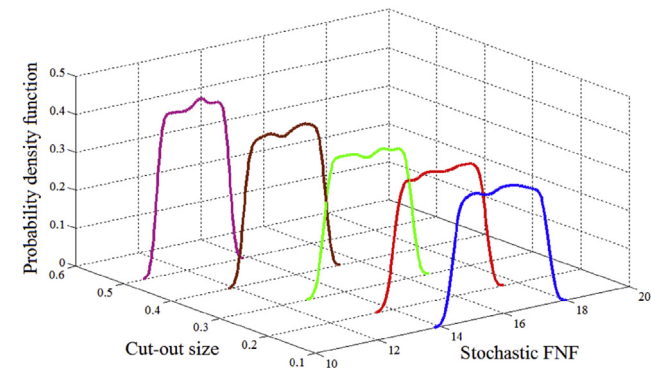
Fig. 7. Probability density function plot for first three stochastic natural frequencies using SVR approach for individual variation of twist angle $[\psi (\bar{\omega})]$ of angle-ply ($45^\circ/-45^\circ/45^\circ$) composite curved panel with cutout.

of fundamental natural frequencies for a simply supported square plate with specific size of the cutout with finite element sizes (4×4) , (8×8) , (12×12) , (16×16) and (20×20) , respectively in addition to comparison with the results obtained by Reddy [65]. Thus, Tables 1 and 2 provide validation of the deterministic finite element model. A discretization of (8×8) mesh on plan area with 64 elements 225 nodes with natural coordinates of an iso-parametric quadratic plate bending element are considered for the present FEM analysis.

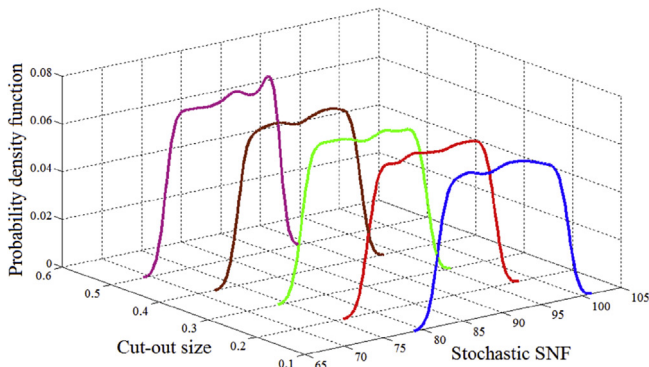
In general, the number of expensive finite element analysis required for original Monte Carlo simulation based UQ approach is

same as the sampling size. The present approach of SVR based uncertainty quantification develops a predictive and representative surrogate model relating each natural frequency to a number of stochastic input parameters.

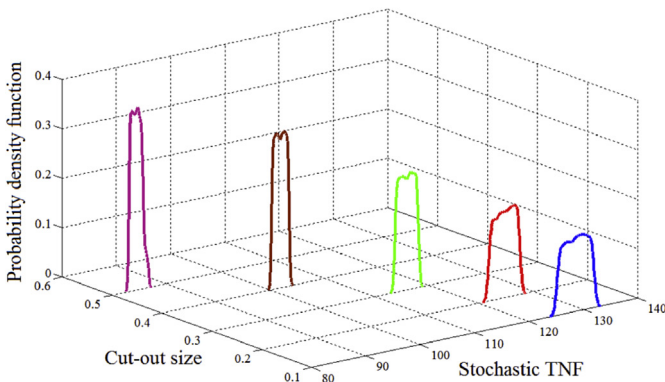
Thus SVR model for a particular mode represents the result encompassing each possible combination of all stochastic input



(a)

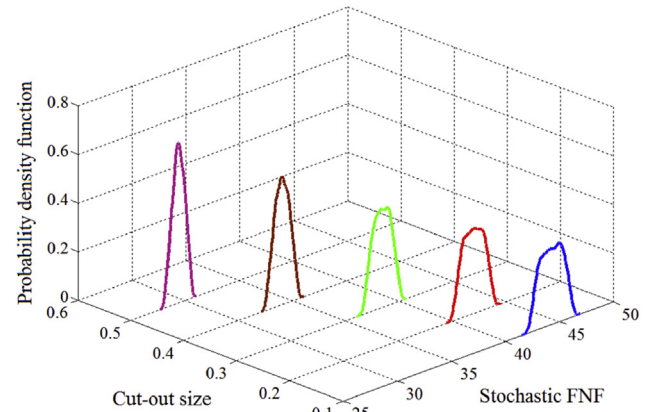


(b)

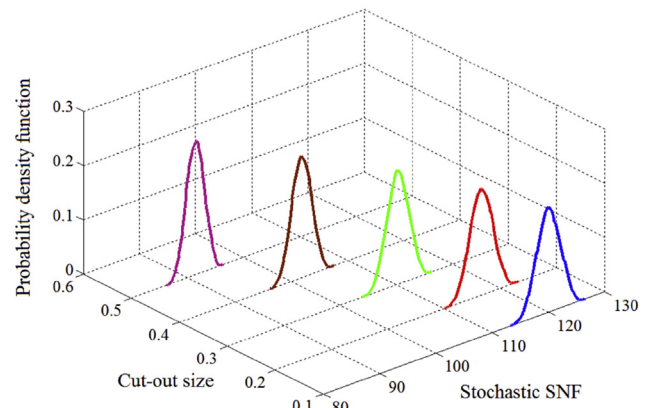


(c)

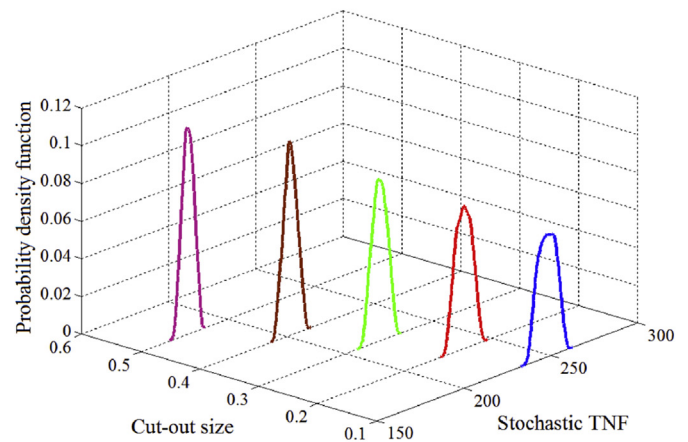
Fig. 8. Probability density function plots for variation of only thickness $[t(\bar{\omega})]$ corresponding to different cut out sizes for composite curved shells with cutout.



(a)



(b)



(c)

Fig. 9. Probability density function plots for variation of only material properties $[p_m(\bar{\omega})]$ corresponding to different cut out sizes for composite curved shells with cutout.

parameters. A convergence study of sample size for SVR model formation with respect to original MCS is tabulated in Table 3 for the first three modes corresponding to individual (ply-orientation angle) and combined variation (ply-orientation angle, twist angle, thickness, elastic moduli, shear moduli, poisson ratio and mass density). By analysing the statistical parameters presented in Table 3 it is evident that sample size of 256 and 512 are adequate for the SVR model formation corresponding to individual and combined cases, respectively. Fig. 4 and Fig. 5 present the scatter plot and probability density function plot, respectively considering the converged sample sizes for stochastic natural frequencies using SVR model and traditional MCS approach for angle-ply (45°/-45°/

45°) composite curved panels with cutout corresponding to individual and for combined variation, respectively. It is evident from these figures that the results of the proposed SVR based approach are in good agreement with that of direct MCS simulations corroborating accuracy and validity of the proposed approach.

The probability density function plots for stochastic first three modes using SVR approach for individual variation of ply orientation angle considering angle-ply ($\theta^\circ/-\theta^\circ/\theta^\circ$) composite curved panels with cutout are presented in Fig. 6. The figure reveals that as

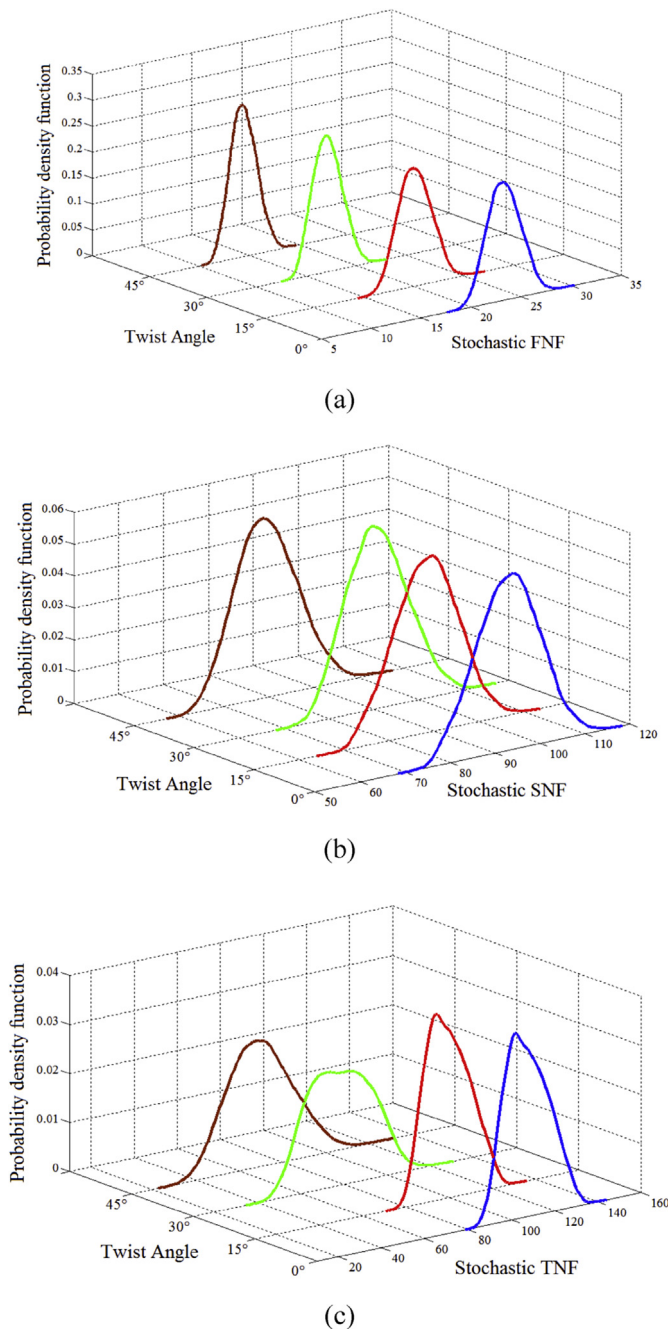


Fig. 10. Probability density function plots for combined variation $[g(\bar{w})]$ corresponding to different twist angle for composite curved shells with cutout.

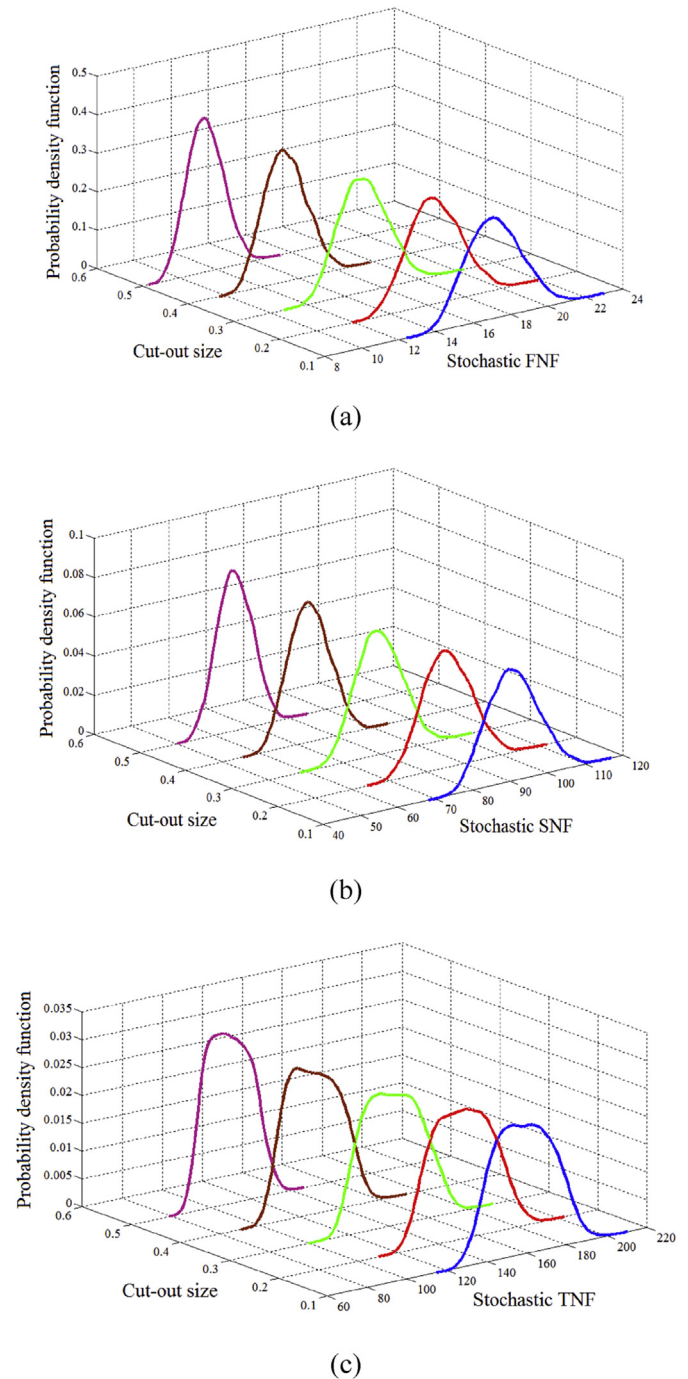


Fig. 11. Probability density function plots for combined variation of ply orientation angle, thickness, twist angle and material properties $[g(\bar{w})]$ corresponding to different cut out sizes for composite curved shells with cutout.

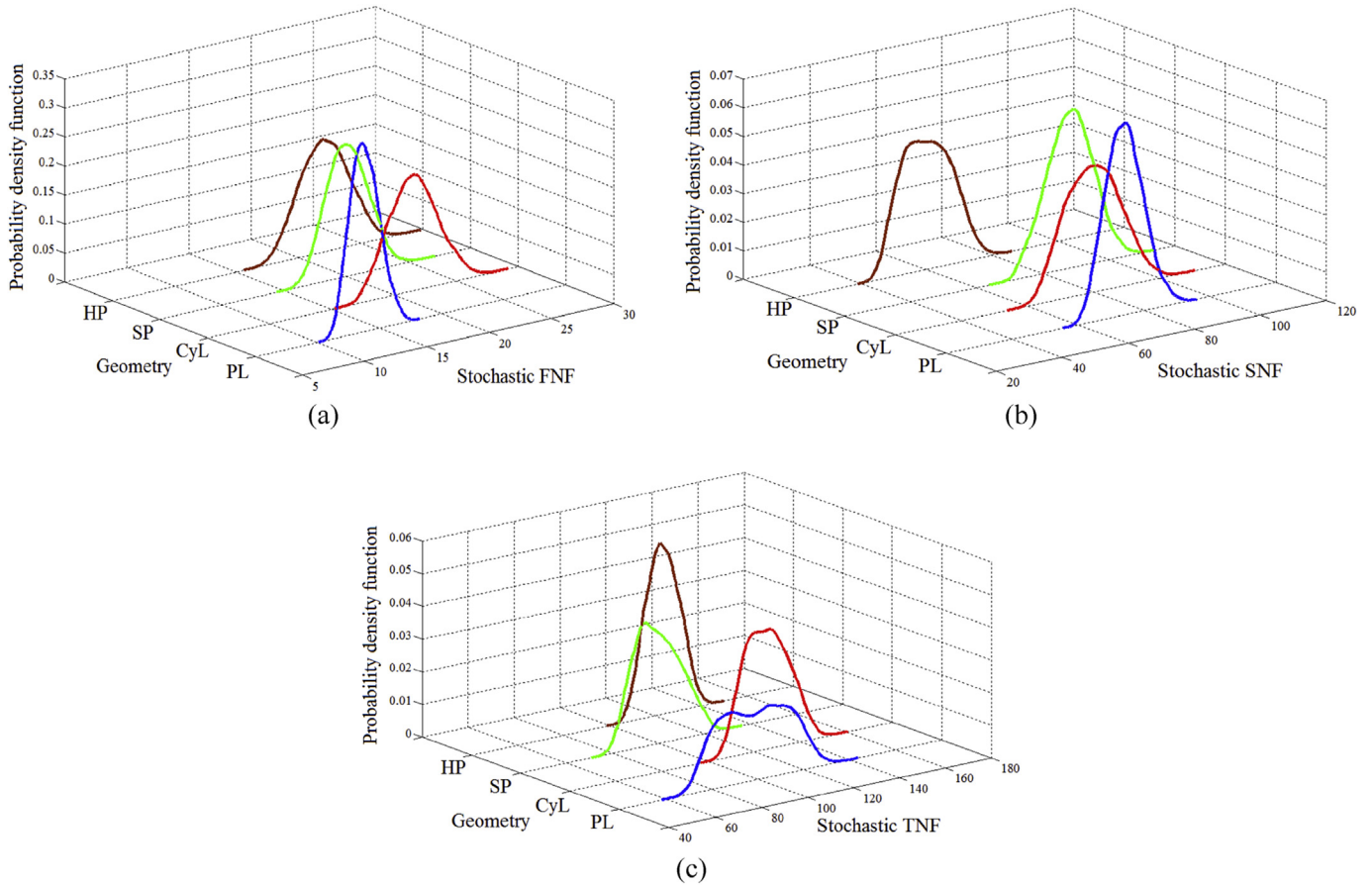


Fig. 12. Probability density function plots for combined variation $[g(\bar{\omega})]$ corresponding to different geometry for composite curved shells with cutout (PL-Plate, CyL-Cylindrical, SP-Spherical, HP-Hyperbolic Paraboloid).

the ply orientation angle (θ) of the angle-ply composite curved panels with a particular size of cutout increases, the stochastic first three natural frequencies are found to reduce. In Figs. 6–12, the first three natural frequencies are referred as fundamental natural frequency (FNF), second natural frequency (SNF) and third natural frequency (TNF) which are stochastic in nature. Fig. 7 presents the probability density function plot for stochastic fundamental natural frequency for individual variation of twist angle only of angle-ply ($45^\circ/-45^\circ/45^\circ$) composite curved panels with cutout. The twist angle in shell-panel structures causes reduction of stiffness which

in turn decreases the values of the first three natural frequencies corresponding to a constant cutout size. The probability distributions of the first three natural frequencies for only variation of thickness corresponding to different sizes of cutout for composite shells are furnished in Fig. 8. The stochastic mean values of first three natural frequencies are found to reduce with increasing cutout size. Fig. 9 presents probability distributions of first three natural frequencies for variation in all the material properties. It is observed that the combined effects of variation of all the material properties follow Gaussian distribution and the mean for all the three natural frequencies reduce with the increase in cutout size.

The probability density function plots of first three modes with combined variation (ply-orientation angle, twist angle, thickness, elastic moduli, shear moduli, poisson ratio and mass density) corresponding to different twist angles are shown in Fig. 10. The mean of stochastic natural frequencies are found to reduce with increase in twist angle. It is interesting to notice that the probabilistic distributions for combined variation (Fig. 10) follow Gaussian distribution, in contrast to the probabilistic characters depicted for individual variation of twist angle only (Fig. 7). Probability distributions for first three modes with combined variation corresponding to different sizes of cutout are shown in Fig. 11, wherein it is evident that the distributions are of Gaussian nature and mean of stochastic natural frequencies decrease with the increase in cutout size. The probability density function plots of the stochastic first three natural frequencies for combined variation corresponding to different geometry such as composite plate, cylindrical, spherical,

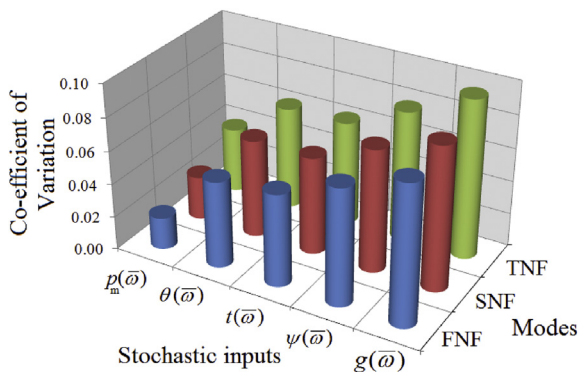


Fig. 13. Coefficient of variation for different of variations of input parameters.

hyperbolic paraboloid curved shells as shown in Fig. 12. Even though the probability distributions are found to follow Gaussian distributions, the mean and standard deviation of natural frequencies for different modes are highly dependent on the type of shell geometry. Fig. 13 presents the coefficient of variation (ratio of standard deviation and mean for a distribution) of the stochastic first three natural frequencies corresponding to individual and combined variation of stochastic input parameters. Coefficient of variation is highest for combined variation of all input parameters, as expected. The analysis presented in Fig. 13 provides a measure of relative sensitivity of different input parameters towards the natural frequencies. Among the stochastic geometric features, twist angle is found to be the most sensitive parameter followed by thickness, ply orientation angle and material properties, respectively.

It is worthy to note here that all the probabilistic results furnished in this paper are obtained on the basis of 10,000 simulations. Application of support vector regression based approach allows us to obtain these results by means of efficient virtual simulations instead of actual expensive finite element simulation. 512 and 256 samples are required to construct the SVR model for layer-wise combined variation and individual variation of the stochastic input parameters, respectively. Thus for the purpose of stochastic analysis, same number of actual FE simulations are needed in the

present approach, in contrast with 10,000 FE simulations needed in traditional MCS based approach. Therefore, the proposed SVR approach for uncertainty quantification is more computationally efficient than traditional MCS approach in terms of FE simulations.

Fig. 14 shows the effect of noise on prediction using SVR considering combined variation of all input parameters. Representative results are presented in Fig. 15 showing the effect of noise on first three natural frequencies considering different levels of noise (p) ranging from 0 to 0.15. The results presented in this paper are obtained on the basis of 1000 such noisy datasets, which involves construction of SVR model and thereby performing MCS for each dataset using corresponding SVR models as explained in Fig. 3(b). A comparative assessment of the effect of different levels of noise with noise free data ($p = 0$) provides a comprehensive idea about the influence of such noise in the probability distributions of first three natural frequencies.

6. Conclusion

This paper presents an efficient support vector regression based stochastic natural frequency analysis for laminated composite curved panels with cutout including the effect of twist angle and variation in shell-panel geometry (such as cylindrical, spherical, hyperbolic paraboloid and plate). First three stochastic natural

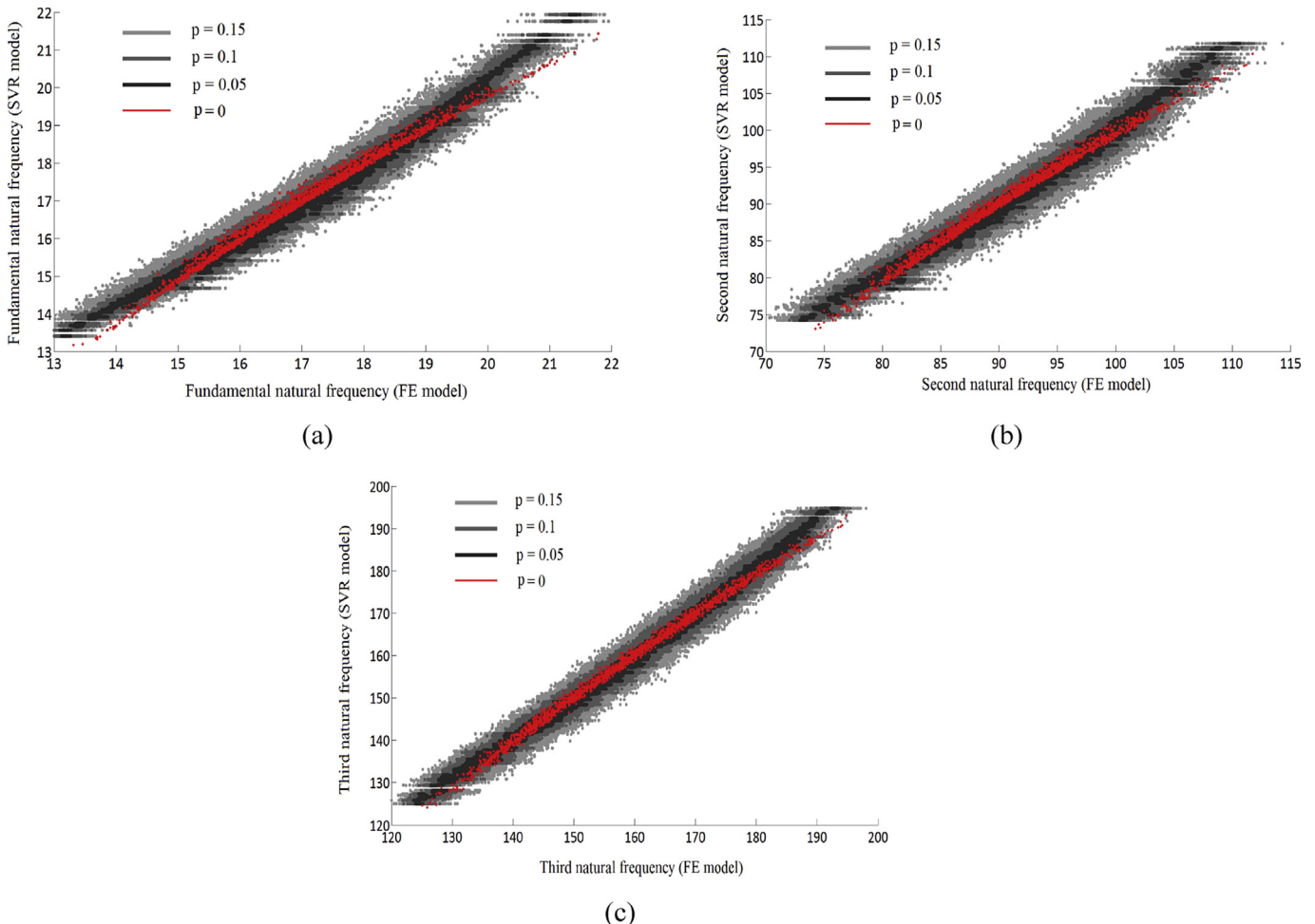


Fig. 14. Effect of noise on prediction capability of SVR model for first three natural frequencies considering combined stochasticity.

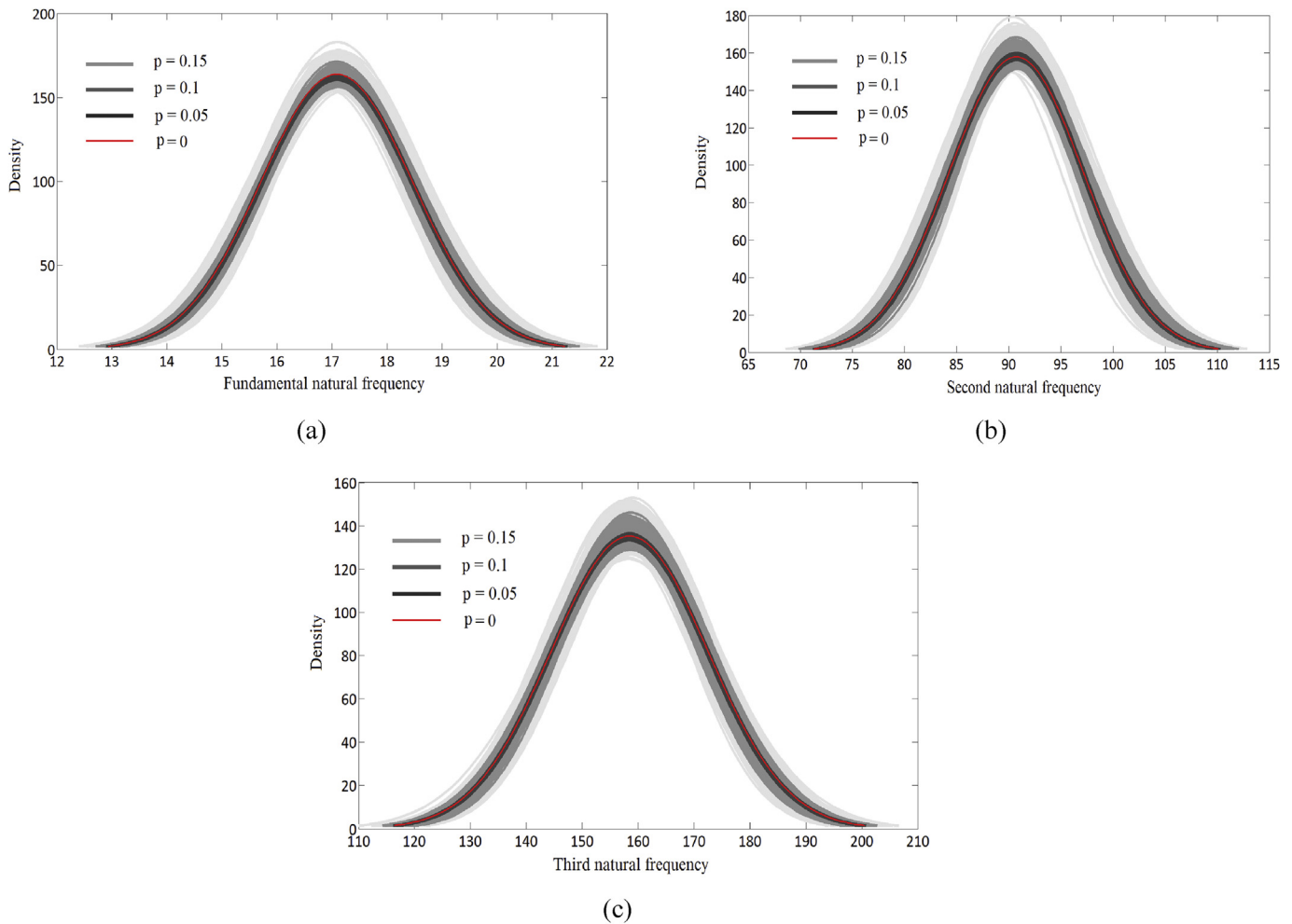


Fig. 15. Effect of noise on SVR based uncertainty quantification algorithm for first three natural frequencies considering combined stochasticity.

frequencies are analyzed considering layer-wise variation of individual (low dimensional input parameter space) as well as combined effect (relatively higher dimensional input parameter space) of random input parameters (such as ply orientation, twist angle, thickness and material properties). The computational time and cost are reduced significantly by using the present SVR based approach compared to traditional Monte Carlo simulation method. A sensitivity analysis among the stochastic material and geometric features is carried out within the analysis domain to ascertain their relative importance. The effect of noise on SVR based uncertainty quantification algorithm in characterizing the probabilistic distribution of natural frequencies is presented to account for the respective variability in practical applications of such structures.

The novelty of the present study includes the stochastic natural frequencies analysis of composite curved panels with cutout and development of the efficient SVR based uncertainty quantification algorithm for laminated composites. Moreover, the effect of noise on SVR based uncertainty quantification algorithm is first analyzed in this article. Even though it is concentrated on stochastic natural frequency analysis of laminated composite curved panels in this paper, the SVR based approach for uncertainty quantification including the effect of noise can be extended to deal with other computationally intensive problems in different fields of science and engineering.

Acknowledgements

TM acknowledges the financial support from Swansea University through the award of Zienkiewicz Scholarship during the period of this work. SA acknowledges the financial support from The Royal Society of London through the Wolfson Research Merit award.

References

- [1] Rajamani A, Prabhakaran R. Dynamic response of composite plates with cut-outs, part I: simply supported plates. *J Sound Vib* 1977a;54(4):549–64.
- [2] Rajamani A, Prabhakaran R. Dynamic response of composite plates with cut-outs, part II: clamped clamped plates. *J Sound Vib* 1977b;54(4):565–76.
- [3] Reddy JN. Large amplitude flexural vibration of layered composite plates with cutouts. *J Sound Vib* 1982;1:1–10.
- [4] Lee HP, Lim SP, Chow ST. Free vibration of composite rectangular plates with rectangular cutouts. *Compos Struct* 1987;8:63–81.
- [5] Lee HP, Lim SP. Free vibration of isotropic and orthotropic square plates with square cut outs subjected to in-plane forces. *Comput Struct* 1992;43(3):431–7.
- [6] Beslin O, Guyader JL. The use of an “ectoplasm” to predict free vibrations of plates with cut-outs. *J Sound Vib* 1996;191(5):935–54.
- [7] Huang M, Sakiyama T. Free vibration analysis of rectangular plates with variously shaped holes. *J Sound Vib* 1999;226(4):769–86.
- [8] Rezaeepazhand J, Jafari N. Stress analysis of perforated composite plates. *Compos Struct* 2005;71:463–8.
- [9] Hota SS, Padhi P. Vibration of plates with arbitrary shapes of cutouts. *J Sound Vib* 2007;302(4–5):1030–6.

- [10] Thornburgh RP, Hilburger MW. A numerical and experimental study of compression-loaded composite panels with cutouts. In: Technical papers – AIAA/ASME/ASCE/AHS/ASC structures, structural dynamics and materials conference 7; May 2006. <http://dx.doi.org/10.2514/6.2006-2004>.
- [11] Dimopoulos CA, Gantes CJ. Numerical methods for the design of cylindrical steel shells with unreinforced or reinforced cutouts. *Thin-Walled Struct* 2015;96:11–28.
- [12] Sai Ram KS, Sreedhar Babu T. Free vibration of composite spherical shell cap with and without a cutout. *Comput Struct* 2002;80(23):1749–56.
- [13] Poore AL, Barut A, Madenci E. Free vibration of laminated cylindrical shells with a circular cutout. *J Sound Vib* 2008;312(1–2):55–73.
- [14] Hu HT, Peng HW. Maximization of fundamental frequency of axially compressed laminated curved panels with cutouts. *Compos Part B Eng* 2013;47:8–25.
- [15] Park T, Lee SY, Voyiadjis GZ. Finite element vibration analysis of composite skew laminates containing delaminations around quadrilateral cutouts. *Compos Part B Eng* 2009;40(3):225–36.
- [16] Malekzadeh P, Bahrinfard F, Ziaee S. Three-dimensional free vibration analysis of functionally graded cylindrical panels with cut-out using Chebyshev–Ritz method. *Compos Struct* 2013;105:1–13.
- [17] Lee SY, Chung DS. Finite element delamination model for vibrating composite spherical shell panels with central cutouts. *Finite Elem Anal Des* 2010;46(3):247–56.
- [18] Parthasarthy G, Ganesan N, Reddy CVR. Study of unconstrained layer damping treatments applied to rectangular plates having central cutouts. *Comput Struct* 1986;23(3):433–43.
- [19] Jenq ST, Hwang GC, Yang SM. The effect of square cut-outs on the natural frequencies and mode shapes of GRP cross-ply laminates. *Compos Sci Technol* 1993;47(1):91–101.
- [20] Eiblmeier J, Loughlan J. The influence of reinforcement ring width on the buckling response of carbon fibre composite panels with circular cut-outs. *Compos Struct* 1997;38(1–4):609–22.
- [21] Sivakumar K, Iyengar NGR, Deb K. Free vibration of laminated composite plates with cutout. *J Sound Vib* 1999;221(3):443–70.
- [22] Anuja G, Katukam R. Parametric studies on the cutouts in heavily loaded aircraft beams. *Mater Today Proc* 2015;2(4–5):1568–76.
- [23] Mondal S, Patra AK, Chakraborty S, Mitra N. Dynamic performance of sandwich composite plates with circular hole/cut-out: a mixed experimental–numerical study. *Compos Struct* 2015;131:479–89.
- [24] Venkatachari A, Natarajan S, Haboussi M, Ganapathi M. Environmental effects on the free vibration of curvilinear fibre composite laminates with cutouts. *Compos Part B Eng* 2016;88:131–8.
- [25] Yu T, Yin S, Bui TQ, Xia S, Tanaka S, Hirose S. NURBS-based isogeometric analysis of buckling and free vibration problems for laminated composites plates with complicated cutouts using a new simple FSDT theory and level set method. *Thin-Walled Struct* 2016;101:141–56.
- [26] Tornabene F, Brischetto S, Fantuzzi N, Viola E. Numerical and exact models for free vibration analysis of cylindrical and spherical shell panels. *Compos Part B Eng* 2015;81:231–50.
- [27] Mukhopadhyay T, Adhikari S. Free vibration analysis of sandwich panels with randomly irregular honeycomb core. *J Eng Mech* 2016. [http://dx.doi.org/10.1061/\(ASCE\)JEM.1943-7889.0001153](http://dx.doi.org/10.1061/(ASCE)JEM.1943-7889.0001153).
- [28] Dey S, Mukhopadhyay T, Spickenheuer A, Gohs U, Adhikari S. Uncertainty quantification in natural frequency of composite plates – an Artificial neural network based approach. *Adv Compos Lett* 2016;25(2):43–8.
- [29] Fantuzzi N, Baccocchi M, Tornabene F, Viola E, Ferreira AJM. Radial basis functions based on differential quadrature method for the free vibration analysis of laminated composite arbitrarily shaped plates. *Compos Part B Eng* 2015;78:65–78.
- [30] Dey S, Mukhopadhyay T, Adhikari S. Stochastic free vibration analyses of composite doubly curved shells – a Kriging model approach. *Compos Part B Eng* 2015;70:99–112.
- [31] Nguyen Khuong D, Nguyen-Xuan H. An isogeometric finite element approach for three-dimensional static and dynamic analysis of functionally graded material plate structures. *Compos Struct* 2015;132:423–39.
- [32] Dey S, Mukhopadhyay T, Sahu SK, Li G, Rabitz H, Adhikari S. Thermal uncertainty quantification in frequency responses of laminated composite plates. *Compos Part B Eng* 2015;80:186–97.
- [33] Yin S, Yu T, Bui Tinh Q, Xia S, Hirose S. A cutout isogeometric analysis for thin laminated composite plates using level sets. *Compos Struct* 2015;127:152–64.
- [34] Dey S, Mukhopadhyay T, Adhikari S. Stochastic free vibration analysis of angle-ply composite plates – a RS-HDMR approach. *Compos Struct* 2015;122:526–36.
- [35] Yu T, Yin S, Bui Tinh Q, Xia S, Tanaka S, Hirose S. NURBS-based isogeometric analysis of buckling and free vibration problems for laminated composites plates with complicated cutouts using a new simple FSDT theory and level set method. *Thin-Walled Struct* 2016;101:141–56.
- [36] Dey S, Mukhopadhyay T, Haddad Khodaparast H, Adhikari S. Stochastic natural frequencies of composite conical shells. *Acta Mech* 2015;226(8):2537–53.
- [37] Fantuzzi N, Tornabene F. Strong formulation isogeometric analysis (SFIGA) for laminated composite arbitrarily shaped plates. *Compos Part B Eng* 2016;96:173–203.
- [38] Dey S, Mukhopadhyay T, Naskar S, Dey TK, Chalak HD, Adhikari S. Probabilistic characterization for dynamics and stability of laminated soft core sandwich plates. *J Sandw Struct Mater* 2016 [Accepted].
- [39] Dey S, Mukhopadhyay T, Haddad Khodaparast H, Adhikari S. Fuzzy uncertainty propagation in composites using Gram-Schmidt polynomial chaos expansion. *Appl Math Model* 2016;40(7–8):4412–28.
- [40] Dey S, Naskar S, Mukhopadhyay T, Spickenheuer A, Bittrich L, Srinivas S, et al. Uncertain natural frequency analysis of composite plates including effect of noise – a polynomial neural network approach. *Compos Struct* 2016;143:130–42.
- [41] Park JS, Kim CG, Hong CS. Stochastic finite element method for laminated composite structures. *J Reinf Plastics Compos* 1995;14(7):7675–93.
- [42] Zhao W, Liu JK, Chen YY. Material behavior modeling with multi-output support vector regression. *Appl Math Model* 2015;39(17):5216–29.
- [43] Sun Zhigang, Wang Changxi, Niu Xuming, Song Yingdong. A response surface approach for reliability analysis of 2.5D C/SiC composites turbine blade. *Compos Part B Eng* 2016;85:277–85.
- [44] Nik Mahdi Arian, Fayazbakhsh Kazem, Pasini Damiano, Lessard Larry. A comparative study of metamodeling methods for the design optimization of variable stiffness composites. *Compos Struct* 2014;107:494–501.
- [45] Steuben J, Michopoulos J, Iliopoulos A, Turner C. Inverse characterization of composite materials via surrogate modeling. *Compos Struct* 2015;132:694–708.
- [46] Zhou XY, Gosling PD, Pearce CJ, Kaczmarczyk L, Ullah Z. Perturbation-based stochastic multi-scale computational homogenization method for the determination of the effective properties of composite materials with random properties. *Comput Methods Appl Mech Eng* 2016;300:84–105.
- [47] Sakata S, Torigoe I. A successive perturbation-based multiscale stochastic analysis method for composite materials. *Finite Elem Anal Des* 2015;102–103:74–84.
- [48] Gao Y, Tong S. Composite adaptive fuzzy output feedback dynamic surface control design for stochastic large-scale nonlinear systems with unknown dead zone. *Neurocomputing* 2016;175(Part A):55–64.
- [49] Kepple J, Herath M, Pearce G, Prusty G, Thomson R, Degenhardt R. Improved stochastic methods for modelling imperfections for buckling analysis of composite cylindrical shells. *Eng Struct* 2015;100:385–98.
- [50] Kollár LP, Springer GS. *Mechanics of composite structures*. Cambridge University Press; 2009.
- [51] Chandrashekhara K. Free vibrations of anisotropic laminated doubly curved shells. *Comput Struct* 1989;33:435–40.
- [52] Meirovitch L. *Dynamics and control of structures*. New York: John Wiley & Sons; 1992.
- [53] Bathe KJ. *Finite element procedures in engineering analysis*. New Delhi: PHI; 1990.
- [54] Fletcher R. *Practical methods of optimization*. New York: John Wiley & Sons; 1989.
- [55] Vapnik VN. *Statistical learning theory*. Wiley; 1998.
- [56] Cherkassky V, Ma Y. Practical selection of SVM parameters and noise estimation for SVM regression. *Neural Netw* 2004;17:113–26.
- [57] Gunn SR. *Support vector machines for classification and regression*. Technical report, image speech and intelligent systems research group. UK: University of Southampton; 1997.
- [58] Mukhopadhyay T, Chowdhury R, Chakrabarti A. Structural damage identification: a random sampling-high dimensional model representation approach. *Adv Struct Eng* 2016. <http://dx.doi.org/10.1177/1369433216630370>.
- [59] Mukhopadhyay T, Naskar S, Dey S, Adhikari S. On quantifying the effect of noise in surrogate based stochastic free vibration analysis of laminated composite shallow shells. *Compos Struct* 2016;140:798–805.
- [60] Mukhopadhyay T, Dey TK, Chowdhury R, Chakrabarti A. Structural damage identification using response surface based multi-objective optimization: a comparative study. *Arab J Sci Eng* 2015;40(4):1027–44.
- [61] Dey S, Mukhopadhyay T, Spickenheuer A, Adhikari S, Heinrich G. Bottom up surrogate based approach for stochastic frequency response analysis of laminated composite plates. *Compos Struct* 2016;140:712–27.
- [62] Mukhopadhyay T, Chakraborty S, Dey S, Adhikari S, Chowdhury R. A critical assessment of Kriging model variants for high-fidelity uncertainty quantification in dynamics of composite shells. *Arch Comput Methods Eng* 2016. <http://dx.doi.org/10.1007/s11831-016-9178-z>.
- [63] Qatu MS, Leissa AW. Natural frequencies for cantilevered doubly curved laminated composite shallow shells. *Compos Struct* 1991;17:227–55.
- [64] Qatu MS, Leissa AW. Vibration studies for laminated composite twisted cantilever plates. *Int J Mech Sci* 1991;33(11):927–40.
- [65] Reddy JN. Large amplitude flexural vibration of layered composite plates with cutouts. *J Sound Vib* 1982;1:1–10.